

## Capturing rare cells from blood using a packed bed of custom-synthesized chitosan microparticles†‡

Cite this: *J. Mater. Chem. B*, 2013, **1**, 4313

Chandamany Arya,<sup>ab</sup> Jason G. Kralj,<sup>b</sup> Kunqiang Jiang,<sup>c</sup> Matthew S. Munson,<sup>b</sup> Thomas P. Forbes,<sup>b</sup> Don L. DeVoe,<sup>d</sup> Srinivasa R. Raghavan<sup>ac</sup> and Samuel P. Forry<sup>\*b</sup>

We describe batch generation of uniform multifunctional chitosan microparticles for isolation of rare cells, such as circulating tumor cells (CTCs), from a sample of whole blood. The chitosan microparticles were produced in large numbers using a simple and inexpensive microtubing arrangement. The particles were functionalized through encapsulation of carbon black, to control autofluorescence, and surface attachment of streptavidin, to enable interactions with biotinylated antibodies. These large custom modified microparticles ( $\approx 164 \mu\text{m}$  diameter) were then packed into a microfluidic channel to demonstrate their utility in rare cell capture. Blood spiked with breast cancer (MCF-7) cells was first treated with a biotinylated antibody (anti-EpCAM, which is selective for cancer cells like MCF-7) and then pumped through the device. In the process, the cancer cells were selectively bound to the microparticles through non-covalent streptavidin–biotin interactions. The number density of captured cells was determined by fluorescence microscopy at physiologically relevant levels. Selective capture of the MCF-7 cells was characterized, and compared favorably with previous approaches. The overall approach using custom synthesized microparticles is versatile, and can allow researchers more flexibility for rare cell capture through simpler and cheaper methods than are currently employed.

Received 7th June 2013

Accepted 1st July 2013

DOI: 10.1039/c3tb20818d

[www.rsc.org/MaterialsB](http://www.rsc.org/MaterialsB)

## 1 Introduction

Recently, there has been much interest in the isolation of rare cells such as circulating tumor cells (CTCs) or stem cells from whole human blood. Rare cell isolation remains a technical challenge, because these cells are present in low numbers relative to red and white blood cells, and has been documented previously.<sup>1–3</sup> The FDA-cleared CTC enumeration technique CellSearch™ relies on paramagnetic beads coated with antibodies to isolate CTCs from blood.<sup>2</sup> Compared to this technique, microfluidic methods promise to increase the capture efficiency due to their higher surface-to-volume ratios;<sup>4</sup> however integration of the functionalized surface necessary for capture can be challenging. One popular microfluidic device for CTC capture relies on an array of antibody-coated posts to enhance

the contacts between cells and antibodies.<sup>3</sup> Newer designs utilize injection molded plastic with similar surface functionalization;<sup>5</sup> however such devices are expensive and/or difficult to construct and custom functionalize (*i.e.* changing the capture antibody) for research studies, especially for researchers who do not have specialized training in surface chemistry and micro-fabrication techniques. For this, custom bead synthesis becomes a viable alternative.

Recently, we introduced a new design wherein near-mono-disperse polystyrene beads (diameter  $\approx 150 \mu\text{m}$ ) with avidin surface functionalization were packed into a bed within a microchannel containing a weir.<sup>6</sup> The beads are commercially available with a surface functionality comprising the linker protein avidin. Pre-stained breast cancer cells were spiked into whole blood as a model CTC sample. After the addition of biotinylated antibody against epithelial cell adhesion molecule (EpCAM), a ligand that is highly expressed on many epithelial cancer cells, this blood was pumped through the packed bed of polystyrene beads. Cells labeled with the biotinylated anti-EpCAM became bound to the beads through biotin–avidin interactions and were enumerated through fluorescence microscopy.

In this paper, we manufactured microparticles for rare cell isolation using the biopolymer chitosan. There were several advantages to working with particles of chitosan compared to polystyrene beads. Specifically, we had greater control over the size, inner contents, and surface properties of the chitosan

<sup>a</sup>Department of Chemical and Biomolecular Engineering, University of Maryland, College Park, MD 20742-2111, USA

<sup>b</sup>Biosystems and Biomaterials Division, NIST, 100 Bureau Dr Gaithersburg, MD 20899, USA. E-mail: [samuel.forry@nist.gov](mailto:samuel.forry@nist.gov); Fax: +1-301-330-3447; Tel: +1-301-975-5246

<sup>c</sup>Department of Chemistry and Biochemistry, University of Maryland, College Park, MD 20742, USA

<sup>d</sup>Department of Mechanical Engineering, University of Maryland, College Park, MD 20742, USA

† Electronic supplementary information (ESI) available. See DOI: 10.1039/c3tb20818d

‡ Official contribution of the National Institute of Standards and Technology; not subject to copyright in the United States.

microparticles. Chitosan is derived from the deacetylation of chitin, a polysaccharide found in the exoskeleton of crustaceans and insects.<sup>7</sup> Chitosan is inexpensive and abundant (chitin is the world's second most common biopolymer<sup>8</sup>), widely commercially available, water soluble below pH 6, and easily functionalized through primary amine groups that allow covalent attachment of enzymes, antibodies, and DNA.<sup>8</sup> The chitosan microparticles were created in-house using a microfluidic tubing device, where two-phase flow generated uniform droplets that template monodisperse microparticles.<sup>9–15</sup> The tubing device allowed uniform particles to be prepared at a throughput of about 5000 particles per hour. The particles were generated continuously in a single step, using a simple and robust method, and no training in microfabrication techniques was necessary. Moreover, chitosan microparticles were easily functionalized by attachment of the protein streptavidin. The core of the microparticles could also be put to use by encapsulating nanoparticles with desired properties. Here, we encapsulated carbon black within the microparticles as a means to attenuate their auto-fluorescence. The final functionalized chitosan microparticles were packed into a bed and used to capture cancer cells spiked into whole blood. Overall, the particles shown here were versatile, utilized inexpensive reagents, and their use within a microfluidic packed bed could prove to be a viable approach for capturing CTCs or other rare cells.

## 2 Experimental section

### Materials and chemicals

Chitosan (medium molecular weight; degree of deacetylation  $\approx$  80%), the nonionic detergent SPAN80, nonpolar solvent hexadecane, the reducing agent sodium cyano-borohydride, the cross linking reagent glutaraldehyde (grade 1, 70%), 1-decanol, phosphate buffer saline (PBS, P4417), albumin from bovine serum (BSA), and streptavidin (from *Streptomyces avidinii*) were obtained from Sigma-Aldrich. Ethyl Alcohol was obtained from Pharmco-AAPER (180 Proof). Carbon black (N110) was obtained from Sid Richardson Carbon Company, fluorescent biotin (Atto 590-Biotin) was obtained from Santa Cruz Biotechnology, small biotinylated polystyrene spheres were purchased from Sphero-tech ((6–8)  $\mu\text{m}$ ), biotinylated anti-EpCAM was purchased from AbCAM (ab79079), and DiI, the fluorescent cell stain, was purchased from Life Technologies (V-22885).<sup>16</sup>

### Tubing device design

Two-phase flow was generated in a microtubing device. Oil and aqueous chitosan solutions were loaded in plastic syringes (BD part # 301030) and pumped through an annular junction as shown in Fig. 1. The aqueous solution was pumped ( $1.5 \mu\text{L min}^{-1}$ ) through silica capillary tubing (i.d.  $150 \mu\text{m}$ , o.d.  $260 \mu\text{m}$ ; SGE Analytical Science), inserted inside PTFE microtubing (i.d.  $300 \mu\text{m}$ ; Cole Parmer), which carried the immiscible oil phase ( $30 \mu\text{L min}^{-1}$ ). Fluidic connections to the silica capillary and PTFE microtubing were made using five-minute epoxy (Devcon) and Luer-lock fittings (1/16" hose barb; Cole Parmer). The rate of aqueous shearing and droplet formation depended on the oil

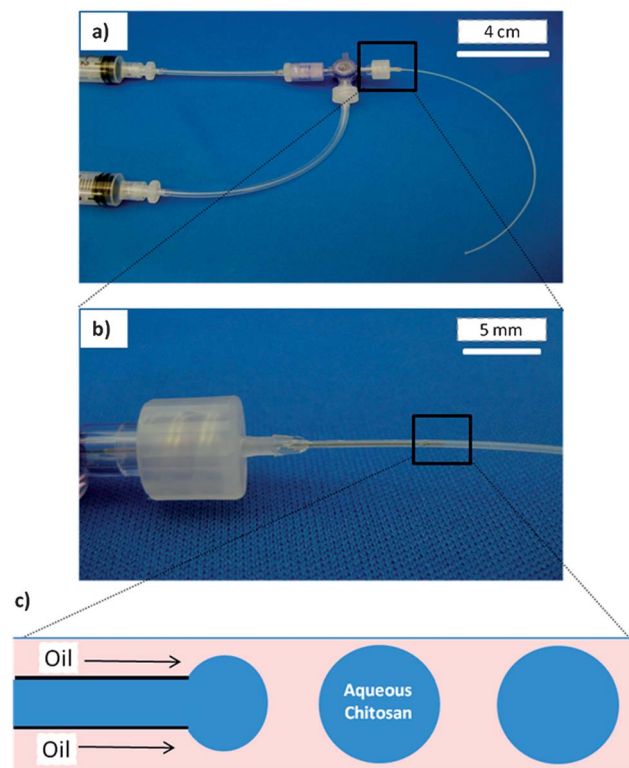


**Fig. 1** Photographs and schematic of the tubing device used to generate chitosan microparticles. The device (a) is formed by inserting capillary microtubing into slightly larger PTFE tubing. A close-up of the device is shown in (b) and a schematic at the junction between the two phases is shown in (c). An aqueous chitosan solution is pumped through the inner tubing. Oil pumped through the outer tubing exerts shear on the aqueous phase at the annular junction, causing uniform microdroplets containing chitosan to break away and flow down the tubing. These microdroplets are collected and cross-linked into uniform microparticles.

and aqueous phase flow rates and was controlled using two independent syringe pumps (New Era Pump Systems Inc.; part # NE-300).

### Chitosan microparticle synthesis

Two-phase flow was generated by a continuous oil phase (2% by weight SPAN80 in hexadecane) and a dispersed aqueous phase (2% by weight chitosan in DI water); flow rates used for the aqueous phase and continuous phase were  $1.5 \mu\text{L min}^{-1}$  and  $30 \mu\text{L min}^{-1}$ , respectively. For generation of carbon black encapsulated chitosan microparticles, the chitosan solution was mixed with 1% by weight carbon black, prior to injection into the syringe. The droplets generated from the tubing device were collected in a cross-linking solution (2% by weight glutaraldehyde, 2% by weight SPAN80 in hexadecane) with gentle stirring. Chitosan droplets were collected over 20 h to generate over  $10^5$  chitosan microparticles. The microparticles were left to incubate in the cross-linking solution over night. They were then washed, by allowing the beads to settle to the bottom of the solution and replacing the existing solution, in a series of solvent exchange steps: pure hexadecane (5 times), 1-decanol (5 times), ethanol (5 times) and PBS (5 times). After washing, the chitosan microparticles did not aggregate and they

also retained their original monodispersity; however, their size shrank by  $\approx 40\%$  through cross-linking and solvent exchange. The final diameters of the chitosan microparticles were measured using brightfield transmission microscopy images. The images were analyzed in MATLAB, using a Hough Transformation to measure their projected diameter.<sup>17</sup> This approach is susceptible to error in determining the absolute particle size (due primarily accurate edge determination), but provides a good assessment of size heterogeneity between particles. The measured sizes from individual microparticles ( $n = 91$ ) were then arranged as a histogram (bin size =  $6.5 \mu\text{m}$ ) in Fig. 2 along with a Gaussian fit to the data.

### Functionalization of chitosan microparticles

Chitosan microparticles in PBS were exposed to glutaraldehyde (8% by weight, 2 h) and washed in PBS (3 times). The microparticles were then exposed to either BSA or streptavidin ( $100 \mu\text{g mL}^{-1}$  in PBS) overnight at  $4^\circ\text{C}$ , and sodium cyano-borohydride (1% by weight, 30 minutes) was added to fix the binding between the chitosan microparticles and streptavidin.<sup>18</sup> Finally the chitosan microparticles were washed in PBS (7 times). Fluorescent intensity was measured on an inverted fluorescent microscope (Axio Observer, DI, Zeiss;  $60\times$  magnification), using a TRITC filter set (excitation at (520–570) nm; emission at (535–675) nm) and compared between samples containing 0% by weight and 1% by weight carbon black as outlined in Fig. 3.

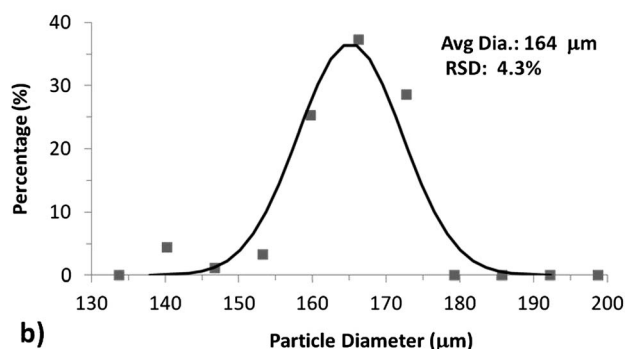
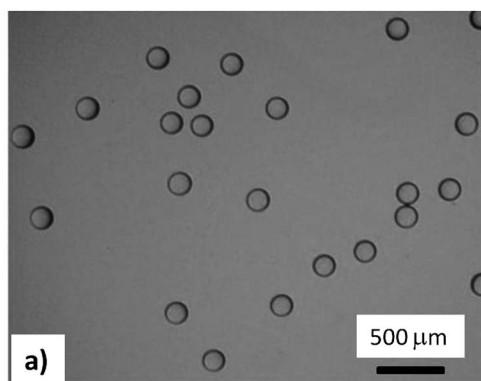


**Fig. 2** Particle sizing. Optical micrographs of chitosan microparticles (a) showed that the particles were uniform and nearly monodisperse. The mean particle diameter (b) was  $\approx 164 \mu\text{m}$  with a relative standard deviation of 4.3% ( $n = 91$ ). The solid line in (b) is a Gaussian fit to the data.

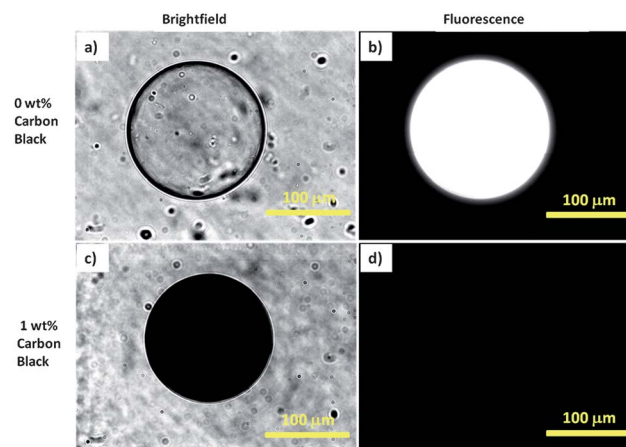


**Fig. 3** Chitosan encapsulation of carbon black nanoparticles. Bare chitosan microparticles cross-linked by glutaraldehyde (a and b) were transparent and exhibited an intrinsic autofluorescence. By encapsulating 1% by weight carbon black (c and d), the microparticles were rendered opaque, and autofluorescence was reduced 50-fold. (Image contrast is identical for b and d.)

Functionalization of the streptavidin was tested using fluorescently labeled biotin. The streptavidin functionalized beads were incubated in a working concentration of  $4 \mu\text{g mL}^{-1}$  Atto-590 biotin, overnight at  $4^\circ\text{C}$ . The beads were washed in PBS ( $7\times$ ) and then the fluorescent intensity was measured using the TRITC filter set. Functionalization at the particle surface was verified by mixing the streptavidin functionalized chitosan microparticles with biotinylated polystyrene microspheres (500 000 beads per mL) on a rotary shaker (90 RPM, 30 min). Similarly, human breast cancer cells (MCF-7, cultured as described previously<sup>6</sup>) were functionalized by incubation with biotinylated anti-EpCAM ( $0.2 \mu\text{g mL}^{-1}$ ) for 30 minutes, and the cells were washed in PBS ( $3\times$ ). Binding of biotinylated cells to streptavidin-functionalized chitosan microparticles was tested (Fig. 4) by mixing the MCF-7 cells (100 000 cells in 1 mL PBS) with the chitosan microparticles on a rotary shaker (90 rpm, 30 minutes).

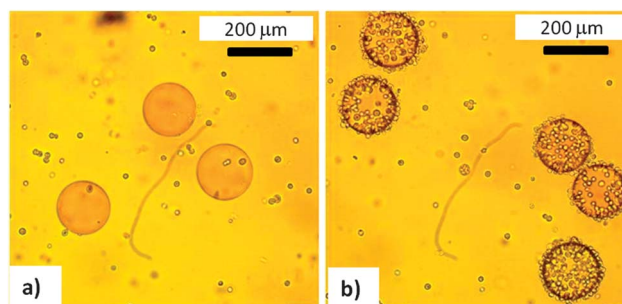


**Fig. 4** Specificity of cell-binding to chitosan microparticles. Chitosan microparticles functionalized with BSA (a) exhibit no specific interaction with biotin covered MCF-7 cells (the MCF-7 cells were treated with biotinylated anti-EpCAM against highly expressed surface proteins). However, streptavidin-functionalized chitosan microparticles (b) are able to capture the same cells due to non-covalent biotin–streptavidin interactions.

### Rare cell capture device and experiments

Streptavidin functionalized chitosan microparticles that encapsulated carbon black were used for the rare cell capture in a microfluidic device. The experiments testing for rare cell capture in a PDMS microfluidic device capture were similar to previous work,<sup>6</sup> except chitosan microparticles were used instead of polystyrene particles. MCF-7 cells were stained with a membrane dye (DiI, Life Technologies), following the manufactures recommendations, and spiked into whole human blood at known densities to mimic clinical CTC samples. Biotinylated anti-EpCAM ( $0.2 \mu\text{g mL}^{-1}$ ) was then added to the blood sample, directly labeling the EpCAM expressing cancer cells for capture on the streptavidin-functionalized microfluidic packed bed. The whole blood samples were then pumped through the microfluidic packed bed. Immobilized MCF-7 cells within the microfluidic packed bed were washed with 200  $\mu\text{L}$  PBS and then identified by fluorescent intensity in ImageJ<sup>19</sup> (see ESI†).

## 3 Results and discussion

### 3.1 Generation of chitosan microparticles

We used a co-flow tubing device made with commercially available tubing (Fig. 1a) to synthesize the chitosan microparticles. Others have reported using similar devices to generate droplets.<sup>20,21</sup> This device allowed a stream of oil (hexadecane) in the annulus region to contact an aqueous stream containing dissolved chitosan in the inner tube. The oil flow sheared the aqueous chitosan solution into uniform spherical droplets (Fig. 1b). The droplet size correlated with the inner diameter of the outer tubing and therefore the size could be varied by appropriate selection of the tubing. Using the tubing device, regular chitosan droplets were formed continuously at a rate of  $\approx 5000$  per hour.

Chitosan droplets were converted to microparticles using glutaraldehyde as the cross-linker similarly to previous microfluidic studies, where chitosan microparticles were manufactured using microfluidic T-junctions.<sup>22</sup> Using the co-flow tubing device, the aqueous chitosan droplets were collected in a solution of glutaraldehyde in hexadecane and were left to cross-link for  $\geq 20$  h. We typically synthesized batches of about  $10^5$  discrete particles. The particles were transferred from the hexadecane phase to an aqueous buffer (phosphate-buffered saline, PBS) by a series of solvent exchange washing steps. In PBS, the particles remained stably dispersed (*i.e.* no aggregation) for over 6 months. Fig. 2a shows a bright-field optical micrograph of the particles. The size distribution determined from these micrographs (Fig. 2b) shows that the particles have a narrow size distribution (4.3% RSD). Thus, our method yields near-monodisperse chitosan microparticles at a reasonably high throughput.

### 3.2 Functionalization of chitosan microparticles

Chitosan microparticles cross-linked with glutaraldehyde exhibit an intrinsic autofluorescence across multiple wavelengths (Fig. 3a and b), as has been noted before.<sup>23,24</sup> Here, the autofluorescence is not a desirable feature since it could interfere with the enumeration of cells by fluorescence microscopy.<sup>25</sup>

Others have shown carbon black, a nanoparticle pigment, as a fluorescence quencher.<sup>26</sup> To attenuate the autofluorescence in the chitosan microparticles, we encapsulated nanoparticles of carbon black (nominal size 12 nm). For this, 1% by weight of carbon black was dispersed in the aqueous chitosan solution used in the tubing device. Chitosan droplets bearing carbon black were cross-linked by glutaraldehyde as before. The resulting microparticles containing carbon black (Fig. 3c and d) were almost completely opaque and showed a 50-fold reduction in detectable autofluorescence across multiple wavelengths. This enabled fluorescent cell detection without interference from the native chitosan autofluorescence (Fig. S1†).

Next, we functionalized the chitosan microparticles with the protein streptavidin. Others have reported covalently anchoring proteins to thin films and beads made from chitosan,<sup>27,28</sup> using glutaraldehyde to attach the chitosan amines to primary amines on the lysine side chains of proteins. As streptavidin is a lysine rich protein, similar chemistry was adopted as previously shown by Dubey *et al.* Since glutaraldehyde was already used here to cross-link the chitosan microparticles, additional glutaraldehyde was added (to completely saturate free amine groups with aldehydes linkages). Subsequent addition of a streptavidin solution yielded streptavidin which was anchored to the chitosan backbone. This was verified by incubating the particles with fluorescently tagged biotin, followed by washing to remove unbound moieties. A significant increase in fluorescence intensity was observed (Fig. S2†), indicating the binding of biotin to attached streptavidin throughout the microparticle volume. For the application of rare cell capture, we were particularly interested in streptavidin functionalization at the microparticle surface. This was tested using micron sized biotinylated spheres; the polystyrene based biotinylated microspheres were too large ((6–8)  $\mu\text{m}$  diameter) to diffuse into the chitosan microparticle, but exhibited significant interaction with streptavidin conjugated to the chitosan microparticle surface (Fig. S3†).

Finally, as a prelude to our rare cell capture experiments, we studied the binding of MCF-7 breast cancer cells to chitosan microparticles in free solution (Fig. 4). The cells were first combined with a biotinylated antibody to EpCAM, which is a ligand that is highly expressed by MCF-7 cells. Cell binding was studied with BSA-functionalized particles (control experiment) as well as streptavidin-functionalized particles (Fig. 4). (Note that, for these studies, particles without carbon black were chosen so as to facilitate visualization in bright-field images.) In the case of the BSA-functionalized particles, little or no binding of biotinylated MCF-7 cells was seen (Fig. 4a). Conversely, the MCF-7 cells substantially cover the surfaces of the streptavidin-functionalized microparticles (Fig. 4b). These studies show that functionalized chitosan microparticles can specifically target biotinylated cells.

### 3.3 Rare cell capture with chitosan microparticles

The device design for rare cell capture was identical to the one reported in our recent paper.<sup>6</sup> Streptavidin-functionalized chitosan microparticles were loaded into the channel in such a way

that the microparticles formed a packed bed (2 mm wide and 15 mm long) against a shallow weir, as shown by the top view in Fig. 5a. A model sample to mimic CTCs in blood was prepared using MCF-7 breast cancer cells labeled with a fluorescent membrane stain. These cells were spiked into whole blood at clinically relevant densities ((0–1000) cells per mL of blood). This sample was then exposed to a biotinylated anti-EpCAM antibody to specifically tag the MCF-7 cells with biotins. Thereafter, the whole blood sample was pumped through the microfluidic packed bed at a flow rate of  $0.2 \text{ mL h}^{-1}$ . Fig. 5b shows a closer fluorescence microscopy image of discrete MCF-7 cells captured in the packed bed. As noted earlier, the autofluorescence of the chitosan microparticles has been sufficiently attenuated so that the captured fluorescently labeled cells showed up as bright spots in the image, which allowed the cells to be counted easily in ImageJ.<sup>19</sup> When the total number of captured cells observed throughout the packed bed was plotted against the number of cells spiked into blood samples, a linear correlation was observed (Fig. 5c). The ratio of these quantities represents the overall capture efficiency and it varied between 21% (Fig. S4†) and 31% (Fig. 5c). For comparison, our earlier packed bed based on polystyrene beads gave similar variability between different blood donors and a capture efficiency of about 40%.<sup>6</sup> We speculate that some of the cells captured by the chitosan-based packed bed could not be

counted because of the opacity of the carbon black in the microparticles – *i.e.*, if the cells were captured on the far side of the microparticles. In general, the majority of cells were captured early in the packed bed and the rate of capture decreased along the length of the packed bed (Fig. S5†). However, capture of rare cells using a packed bed of chitosan beads was not fully optimized in this pilot study. Future experiments to increase capture efficiency could involve tuning the microparticle size, flow rates, and packing length.

Overall, these results demonstrate a promising utility of functionalized chitosan microparticles for rare cell capture. Our calculations show that a single batch of  $10^5$  chitosan microparticles prepared using our tubing device is sufficient to fill over 50 packed beds like the one shown in Fig. 5. This process was not fully optimized, but based on the costs of the materials (not including labor), this translates into a cost of  $\approx \$1.50$  per packed bed of chitosan particles; for comparison, a similar packed bed of commercially available streptavidin-coated polystyrene beads costs  $\approx \$25$ . Moreover, for clinical tests, the packed beds would need to process standard blood draws (7.5 mL) in 1 hour, which would require at least an order of magnitude more beads, thereby magnifying the costs for use. In applications where the high cost of commercial polystyrene beads may be prohibitive, simple methods for batch generation of beads may be preferred. Many bead materials including

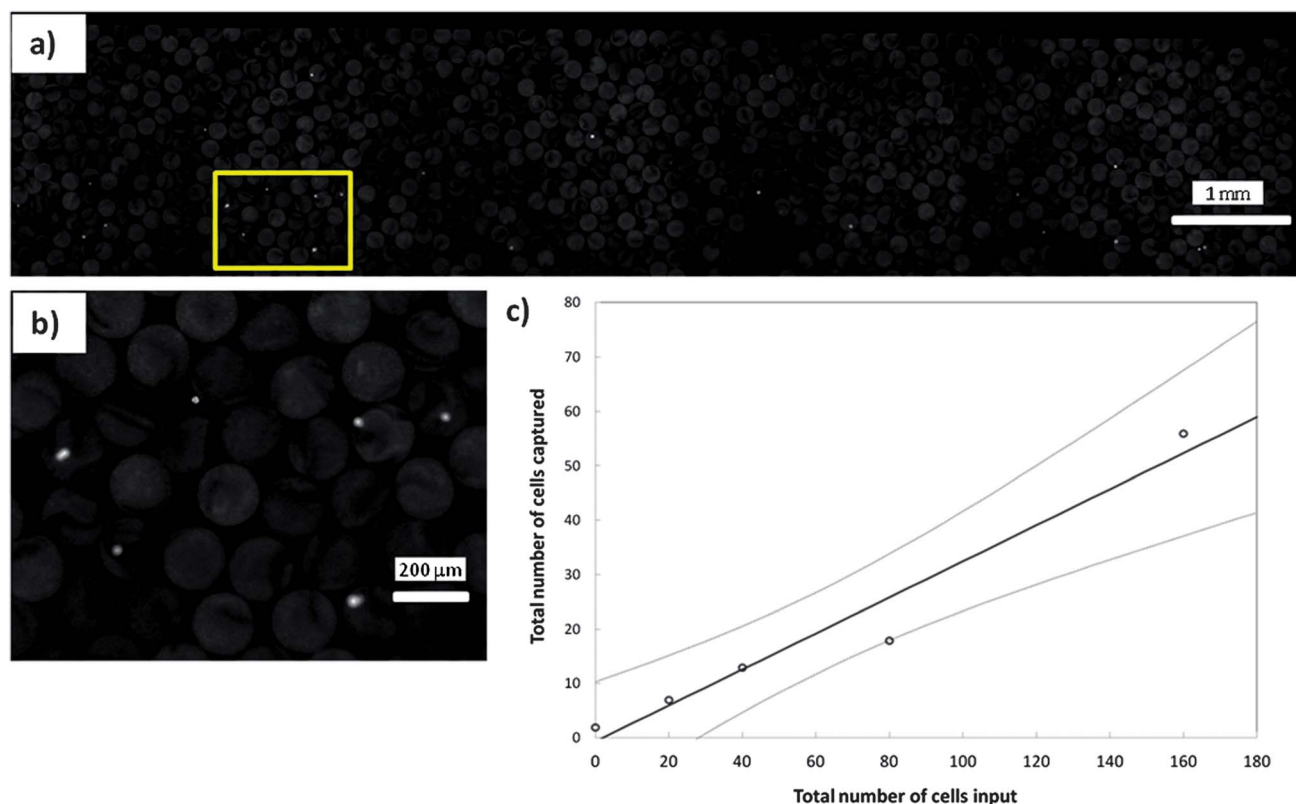


**Fig. 5** Capture of cancer cells from whole blood. The streptavidin functionalized chitosan microparticles were loaded into a microfluidic channel. The uniform size of the microparticles led to the generation of a uniform packed bed (a). After pumping through model CTC blood samples (200  $\mu\text{L}$ ), captured cancer cells were imaged by fluorescence microscopy (b; expanded view of the rectangle in (a)). The total number of cancer cells captured and enumerated in the packed bed exhibited a linear response across the physiologically relevant range (c). A linear regression and Working-Hotelling 95% confidence bands are shown; capture efficiency was  $\approx 31\%$ .

common biopolymers (e.g. alginate) and synthetic polymers<sup>29</sup> could be used. Chitosan is presented here as an attractive alternative that is not only inexpensive, but contains free amine groups that allow for simple chemistry and surface functionalization.

## 4 Conclusions and outlook

We have utilized a simple tubing-based device and method for bulk generation of uniform custom-functionalized, non-fluorescent chitosan microparticles. These devices were quickly and easily assembled using inexpensive and commercially available microtubing. Microparticle properties were modulated through both physical encapsulation of carbon black and attachment of streptavidin: inclusion of carbon black provided a means to attenuate the intrinsic autofluorescence of the microparticles; attachment of streptavidin was shown to allow selective binding to biotinylated surfaces. The utility of the inexpensive production of uniform chitosan microparticles in bulk was demonstrated by loading microfluidic packed beds with functionalized microparticles for studies in rare cell capture. Model cancer cells (MCF-7) were isolated from whole blood at physiologically relevant levels. In comparison to the polystyrene microparticles used previously, chitosan microparticles were more than an order of magnitude cheaper and could offer unique advantages as a tunable biopolymer-based material. Future studies on optimization of the chitosan capture system through adjusting bead sizes and surface functionality could allow for higher capture efficiencies. The versatility of custom synthesized chitosan microparticles allows for generation of more advanced capture devices. For example, alternate capture antibodies could allow isolation of other types of rare cells such as hematopoietic stem cells (HSCs),<sup>30</sup> and the incorporation of magnetic nanoparticles could allow magnetic manipulation of the chitosan microparticles. The overall flexibility in batch generation of custom chitosan microparticles may offer useful means for researchers interested in rare cell isolation through the simplest, inexpensive, and most accessible methods possible.

## References

- 1 Y. Y. Ng, M. R. Baert, E. F. de Haas, K. Pike-Overzet and F. J. Staal, Isolation of human and mouse hematopoietic stem cells, *Methods Mol. Biol.*, 2009, **506**, 13–21.
- 2 J. den Toonder, Circulating tumor cells: the Grand Challenge, *Lab Chip*, 2011, **11**, 375–377.
- 3 S. Nagrath, L. V. Sequist, S. Maheswaran, D. W. Bell, D. Irimia, L. Ulkus, M. R. Smith, E. L. Kwak, S. Digumarthy, A. Muzikansky, P. Ryan, U. J. Balis, R. G. Tompkins, D. A. Haber and M. Toner, Isolation of rare circulating tumour cells in cancer patients by microchip technology, *Nature*, 2007, **450**, 1235–1239.
- 4 A. Hatch, G. Hansmann and S. K. Murthy, Engineered Alginate Hydrogels for Effective Microfluidic Capture and Release of Endothelial Progenitor Cells from Whole Blood, *Langmuir*, 2011, **27**, 4257–4264.
- 5 S. L. Stott, C. H. Hsu, D. I. Tsukrov, M. Yu, D. T. Miyamoto, B. A. Waltman, S. M. Rothenberg, A. M. Shah, M. E. Smas, G. K. Korir, F. P. Floyd, A. J. Gilman, J. B. Lord, D. Winokur, S. Springer, D. Irimia, S. Nagrath, L. V. Sequist, R. J. Lee, K. J. Isselbacher, S. Maheswaran, D. A. Haber and M. Toner, Isolation of circulating tumor cells using a microvortex-generating herringbone-chip, *Proc. Natl. Acad. Sci. U. S. A.*, 2010, **107**, 18392–18397.
- 6 J. G. Kralj, C. Arya, A. Tona, T. P. Forbes, M. S. Munson, L. Sorbara, S. Srivastava and S. P. Forry, A simple packed bed device for antibody labelled rare cell capture from whole blood, *Lab Chip*, 2012, **12**, 4972–4975.
- 7 G. F. Payne and S. R. Raghavan, Chitosan: a soft interconnect for hierarchical assembly of nano-scale components, *Soft Matter*, 2007, **3**, 521–527.
- 8 S. T. Koev, P. H. Dykstra, X. Luo, G. W. Rubloff, W. E. Bentley, G. F. Payne and R. Ghodssi, Chitosan: an integrative biomaterial for lab-on-a-chip devices, *Lab Chip*, 2010, **10**, 3026–3042.
- 9 T. Nisisako, T. Torii and T. Higuchi, Novel microreactors for functional polymer beads, *Chem. Eng. J.*, 2004, **101**, 23–29.
- 10 B. G. De Geest, J. P. Urbanski, T. Thorsen, J. Demeester and S. C. De Smedt, Synthesis of monodisperse biodegradable microgels in microfluidic devices, *Langmuir*, 2005, **21**, 10275–10279.
- 11 S. Seiffert and D. A. Weitz, Controlled fabrication of polymer microgels by polymer-analogous gelation in droplet microfluidics, *Soft Matter*, 2010, **6**, 3184–3190.
- 12 W. J. Duncanson, T. Lin, A. R. Abate, S. Seiffert, R. K. Shah and D. A. Weitz, Microfluidic synthesis of advanced microparticles for encapsulation and controlled release, *Lab Chip*, 2012, **12**, 2135–2145.
- 13 N. Lorber, F. Sarrazin, P. Guillot, P. Panizza, A. Colin, B. Pavageau, C. Hany, P. Maestro, S. Marre, T. Delclos, C. Aymonier, P. Subra, L. Prat, C. Gourdon and E. Mignard, Some recent advances in the design and the use of miniaturized droplet-based continuous process: Applications in chemistry and high-pressure microflows, *Lab Chip*, 2011, **11**, 779–787.
- 14 C. N. Baroud, F. Gallaire and R. Dangla, Dynamics of microfluidic droplets, *Lab Chip*, 2010, **10**, 2032–2045.
- 15 R. Seemann, M. Brinkmann, T. Pfohl and S. Herminghaus, Droplet based microfluidics, *Rep. Prog. Phys.*, 2012, **75**, 016601.
- 16 Certain commercial products are identified in order to adequately specify the experimental procedure; this does not imply endorsement or recommendation by NIST.
- 17 D. H. Ballard, Generalizing the Hough Transform to Detect Arbitrary Shapes, *Pattern Recogn.*, 1981, **13**, 111–122.
- 18 C. D. Meyer, C. S. Joiner and J. F. Stoddart, Template-directed synthesis employing reversible imine bond formation, *Chem. Soc. Rev.*, 2007, **36**, 1705–1723.
- 19 W. S. Rasband, ImageJ, US National Institutes of Health, <http://imagej.nih.gov/ij/>, 1997–2012.
- 20 E. Quevedo, J. Steinbacher and D. T. McQuade, Interfacial polymerization within a simplified microfluidic device: Capturing capsules, *J. Am. Chem. Soc.*, 2005, **127**, 10498–10499.

- 21 G. Nurumbetov, N. Ballard and S. A. F. Bon, A simple microfluidic device for fabrication of double emulsion droplets and polymer microcapsules, *Polym. Chem.*, 2012, **3**, 1043–1047.
- 22 K. Q. Jiang, C. Xue, C. D. Arya, C. R. Shao, E. O. George, D. L. DeVoe and S. R. Raghavan, A New Approach to In-Situ “Micromanufacturing”: Microfluidic Fabrication of Magnetic and Fluorescent Chains Using Chitosan Microparticles as Building Blocks, *Small*, 2011, **7**, 2470–2476.
- 23 W. Wei, L. Y. Wang, L. Yuan, X. D. Yang, Z. G. Su and G. H. Ma, Bioprocess of uniform-sized crosslinked chitosan microspheres in rats following oral administration, *Eur. J. Pharm. Biopharm.*, 2008, **69**, 878–886.
- 24 W. Wei, L. Y. Wang, L. Yuan, Q. Wei, X. D. Yang, Z. G. Su and G. H. Ma, Preparation and application of novel microspheres possessing autofluorescent properties, *Adv. Funct. Mater.*, 2007, **17**, 3153–3158.
- 25 V. C. Oliveira, R. C. V. Carrara, D. L. C. Simoes, F. P. Saggiaro, C. G. Carlotti, D. T. Covas and L. Neder, Sudan Black B treatment reduces autofluorescence and improves resolution of *in situ* hybridization specific fluorescent signals of brain sections, *Histol. Histopathol.*, 2010, **25**, 1017–1024.
- 26 N. S. Allen, J. M. Pena, M. Edge and C. M. Liauw, Behaviour of carbon black pigments as excited state quenchers in LDPE, *Polym. Degrad. Stab.*, 2000, **67**, 563–566.
- 27 X. W. Shi, Y. Liu, A. T. Lewandowski, L. Q. Wu, H. C. Wu, R. Ghodssi, G. W. Rubloff, W. E. Bentley and G. F. Payne, Chitosan biotinylation and electrodeposition for selective protein assembly, *Macromol. Biosci.*, 2008, **8**, 451–457.
- 28 A. N. Singh, S. Singh, N. Suthar and V. K. Dubey, Glutaraldehyde-Activated Chitosan Matrix for Immobilization of a Novel Cysteine Protease, Procerain B, *J. Agric. Food Chem.*, 2011, **59**, 6256–6262.
- 29 K. Q. Jiang, A. Sposito, J. K. Liu, S. R. Raghavan and D. L. DeVoe, Microfluidic synthesis of macroporous polymer immunobeads, *Polymer*, 2012, **53**, 5469–5475.
- 30 L. Gallacher, B. Murdoch, D. M. Wu, F. N. Karanu, M. Keeney and M. Bhatia, Isolation and characterization of human CD34(–)Lin(–) and CD34(+ )Lin(–) hematopoietic stem cells using cell surface markers AC133 and CD7, *Blood*, 2000, **95**, 2813–2820.

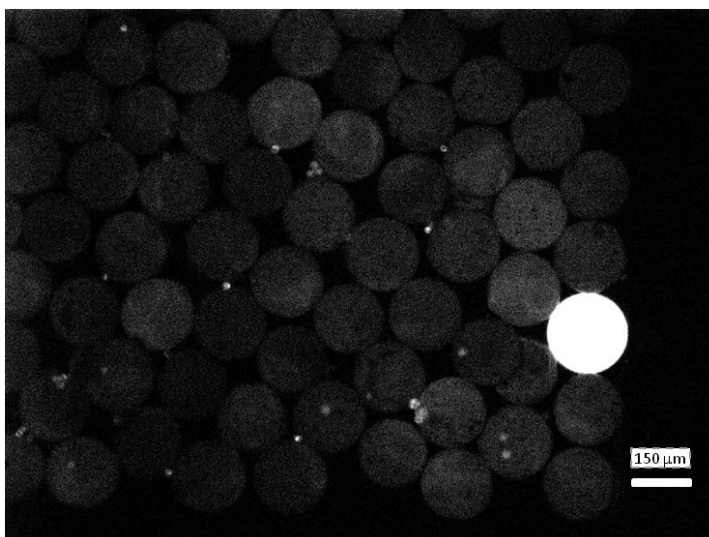


**Figure S1.** Fluorescent image of DiI-stained cells and chitosan microparticles (diameter  $\approx 164 \mu\text{m}$ ). The chitosan microparticles were loaded with 1% by weight carbon black to attenuate their intrinsic autofluorescence. The one bright microparticle contained no carbon black and emitted a strong autofluorescence that was much brighter than the microparticles encapsulating carbon black or fluorescently stained cells. This image was taken using an inverted fluorescent microscope and a TRITC filter set (Ex: 520-570; Em: 535-675) at 10 $\times$  magnification.

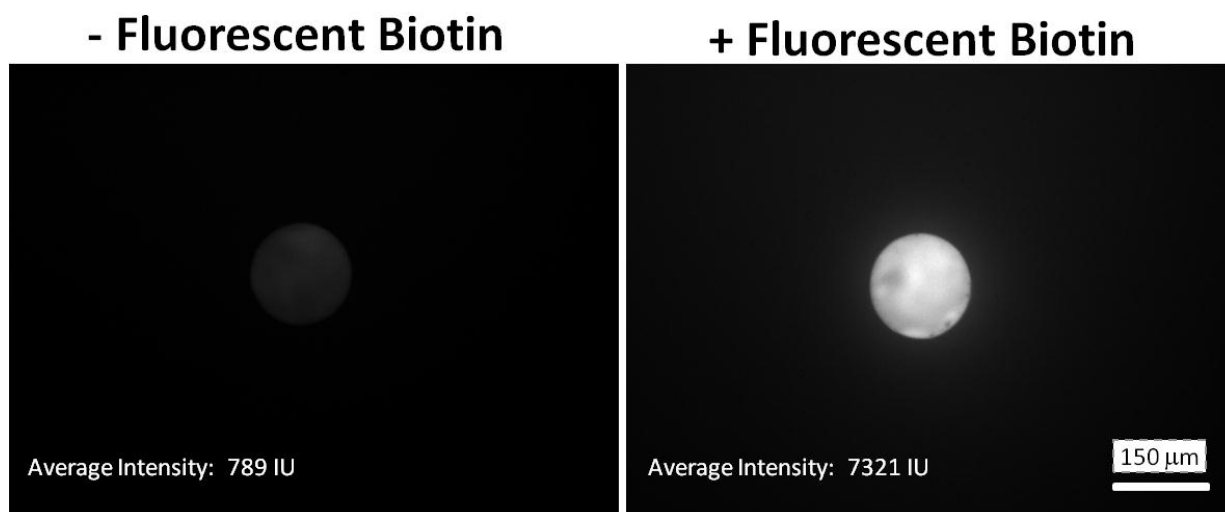


**Figure S2.** Fluorescent biotin increased the fluorescent intensity of streptavidin-functionalized chitosan microparticles. The chitosan microparticles, which encapsulated 1% by weight carbon black, were covalently functionalized with streptavidin. Following exposure to fluorescent biotin in solution followed by washing, a significant increase in fluorescent intensity was observed. These images were taken using an inverted fluorescent microscope and a TRITC filter set (Ex: 520-570; Em: 535-675) at 10 $\times$  magnification.



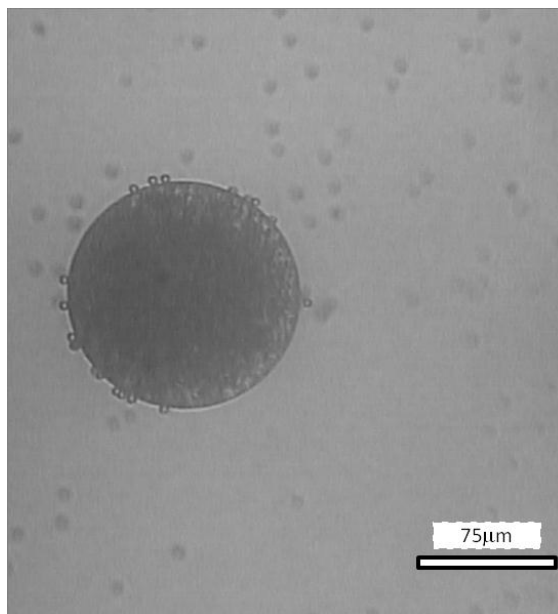


**Figure S3.** Attachment of small biotinylated polystyrene spheres (6-8  $\mu\text{m}$ ) to streptavidin-functionalized chitosan microparticles. When chitosan microparticles were mixed with the commercially available biotinylated polystyrene spheres, significant surface attachment of the spheres to the chitosan microparticle demonstrated that covalently bound streptavidin was present at the microparticle surface.

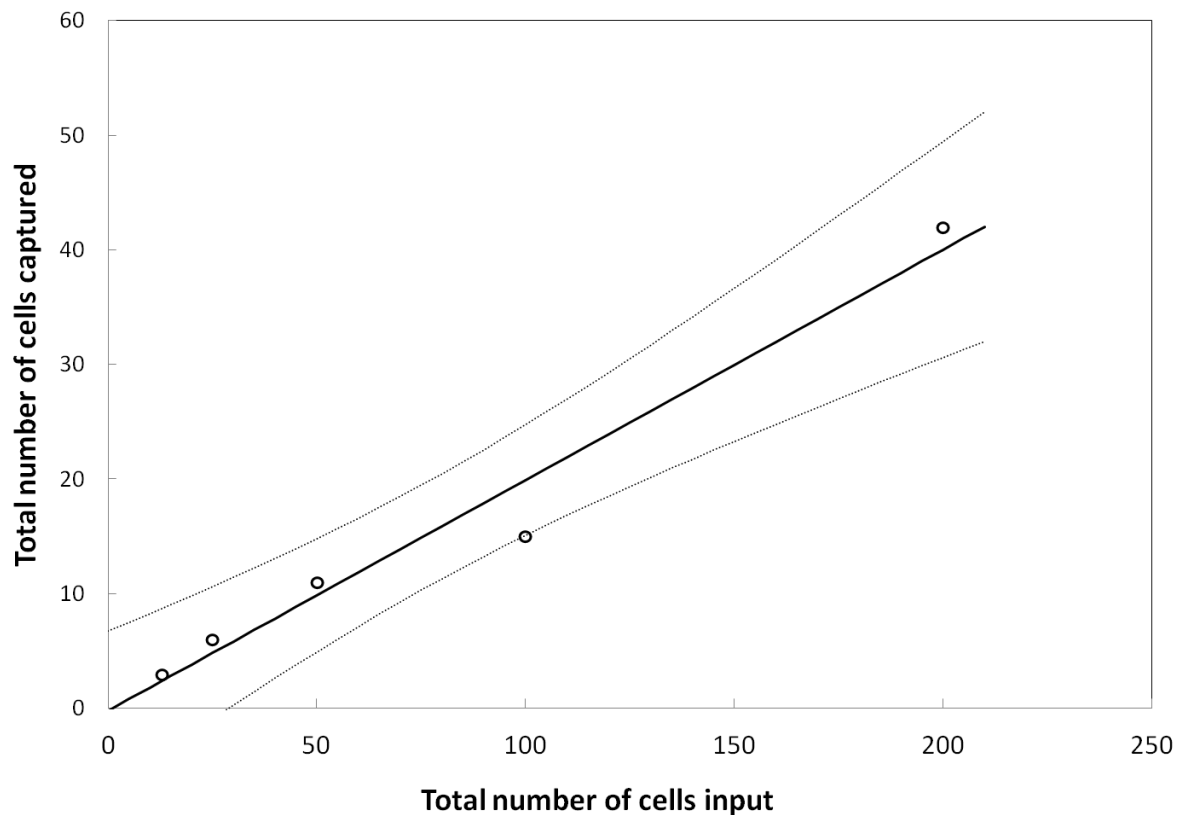


**Figure S4.** Additional CTC model samples (MCF-7 cells spiked into whole blood) analyzed using the microfluidic packed bed. The total number of cancer cells captured and enumerated in the packed bed exhibited a linear response across the physiologically relevant range with a capture efficiency  $\approx 21\%$ . This experiment was identical to the one shown in Figure 5, except that the whole blood was collected from a different healthy donor. This system response is identical to our previous work.

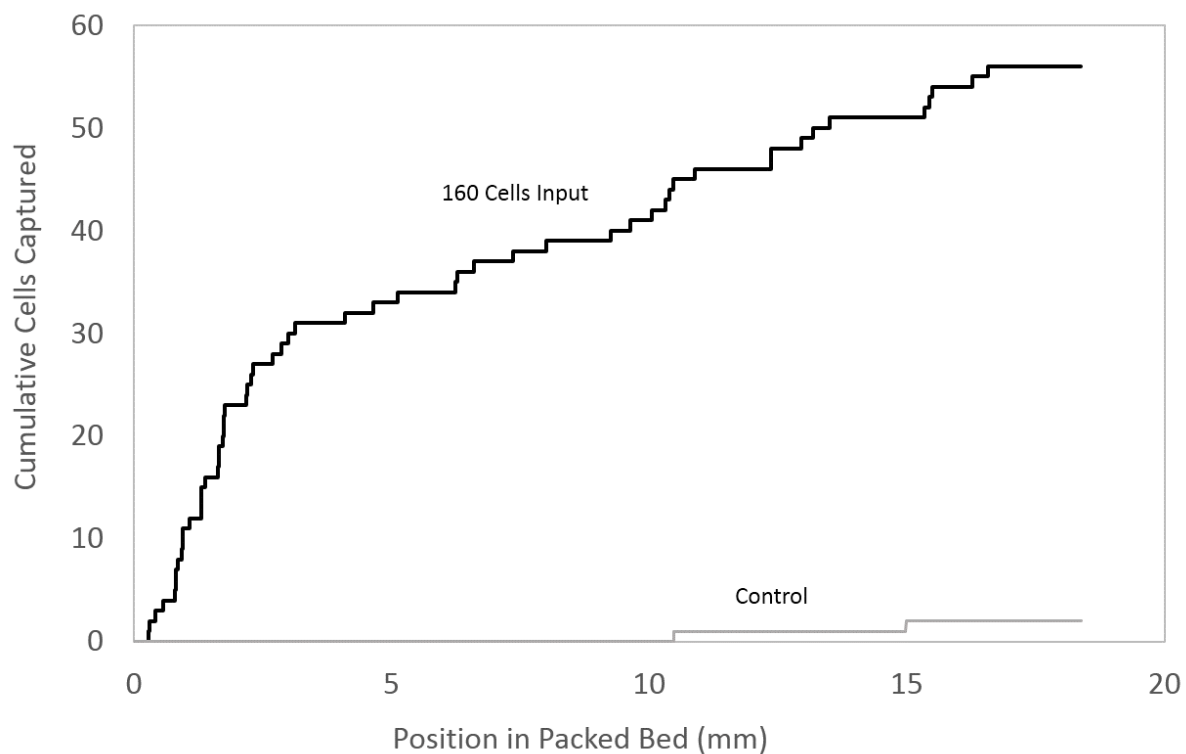


**Figure S5.** Cumulative cells captured as a function of position in the packed bed. The top line represents data from a single capture experiment (figure 5C) where 160 MCF-7 cells were spiked into 200  $\mu\text{L}$  whole blood and run through the packed bed of chitosan beads. The bottom line shows results of the control run where 200  $\mu\text{L}$  of whole blood that did not contain any MCF-7 cells were run through the packed bed.

## Enumeration of Captured Cells for Figure 5:

DiI stained cancer cells were captured using a packed bed of chitosan microspheres as described in Figure 5. To analyze the data in Figure 5, fluorescent images of the column were taken using two different filter sets. The first filter cube (a; TRITC: excitation at (520-570) nm and emission at (535-675) nm) overlapped with the excitation and emission of membrane cell stain (DiI: excitation peak  $\approx$  549 nm; emission peak  $\approx$  565 nm). The second filter set (b; FITC: excitation at (450-490) nm and emission at (515-565) nm) did not detect the cell stain. The chitosan microspheres exhibited a broadband autofluorescence that was detected in both filter sets. Thus, the difference between the filter sets (c) allowed facile enumeration of the cells. Overlapping images at each point along the packed beds were manually stitched together (e.g. Figure 5a) and the cells were counted (e.g. Figure 5c; Figure S4) using a simple fluorescent intensity threshold in ImageJ.

